Nonrenewable Resources, Vol. 7, No. 1, 1998

Zonation in Primary Halos and Geochemical Prospecting Pattern for the Guilaizhuang Gold Deposit, Eastern China

Chen Yongqing[1] and Zhao Pengda[1,2]

Received November 27, 1996, accepted January 22, 1997

The Guilaizhuang gold deposit, with an average grade of 8.10 g/t Au and reserves of over 30 mt, is a subvolcanic epithermal deposit. The deposit is hosted in Paleozoic carbonate rocks in the western Shandong metallogenic terrane of the littorine Pacific metallogenic domain, eastern China, and is associated spatially with an early Mesozoic subvolcanic alkalic intrusive complex (188–190 Ma). The orebody was discovered at the end of the 1980s based on anomalies of Au in stream sediment samples at a map scale of 1:200,000. The ore is rich in Au, Ag, Te, V, F, As, Sb, Tl, W, and Mo but poor in Cu, Pb, and Zn. The ore is similar in its trace elements to Carlin-type Au deposits. The transverse element association zonation of the deposit is as follows: (on the hanging wall) F ⇐ W–Mo–As–Tl ⇐ Se–Sb–Bi ⇐ Au–Ag–Te (orebody) ⇒ Se–Sb–Bi (on the foot wall). The axial zonation is as follows: Au ⇒ Ag ⇒ Sb ⇒ V ⇒ Zn ⇒ W ⇒ F ⇒ Mo ⇒ Tl ⇒ As. Indexes such as $(Au + Sb)_D$ / $(As + Tl)_D$ and $(Au + Ag)_D/(As + Tl)_D$ decrease with depth but dramatically increase at the level where the orebody pinches out, which indicates another orebody might exist at depth. Multivariate statistical analysis suggests that the ore (halo)-forming process can be divided into two stages: alteration and mineralization. The former includes: potash feldsparization, albitization, silicification, and fluoritization. The latter includes the following substages: arsenopyritization and scheelitization; pyritization, chalcopyritization, and sphaleritization; and native gold, electrum, and calaveritization. The last substage is considered to be the main ore-forming stage in the formation of the deposit.

KEY WORDS: Transverse zonation of element association; axial zonation in primary halos; geochemical prospecting pattern; epithermal gold deposit; alkalic intrusive rocks.

INTRODUCTION

The Guilaizhuang gold deposit is a buried subvolcanic epithermal ore deposit. It is located at the southwest edge of the Pingyi-Feixian Mesozoic tectonovolcanic basin in the western Shandong metallogenic terrane of the littorine Pacific metallogenic domain, eastern China, and is spatially associated with the subvolcanic alkalic intrusive complex emplaced in Archean metamorphic green rocks and Paleozoic carbonate rocks. The geologic setting of the deposit is shown in figure 1 (Quan, 1992; Qiu and others, 1994; Lin and others, 1995; Chen and others, 1995; Jin and Shen, 1995; Yu, 1996). Initially, it was concluded that the gold was not associated with the alkalic intrusive rocks. More recently, however, a number of large gold deposits have been found to be associated with alkalic complexes, such as Kirkland Lake, Canada; Cripple Creek, Colorado; Mount Kare in the highlands of Papua Guinea; Dongping, north China since the 1980s, (Richards and Ledlie, 1993; Xiang and Ye, 1995; Liang, 1995). For this reason, it was necessary not only to reconsider the initial conclusion but also to study the

[1] Institute of Mathematical Geology and Remote Sensing Geology, China University of Geosciences, Wuhan 430074, China.
[2] To whom correspondence should be sent.

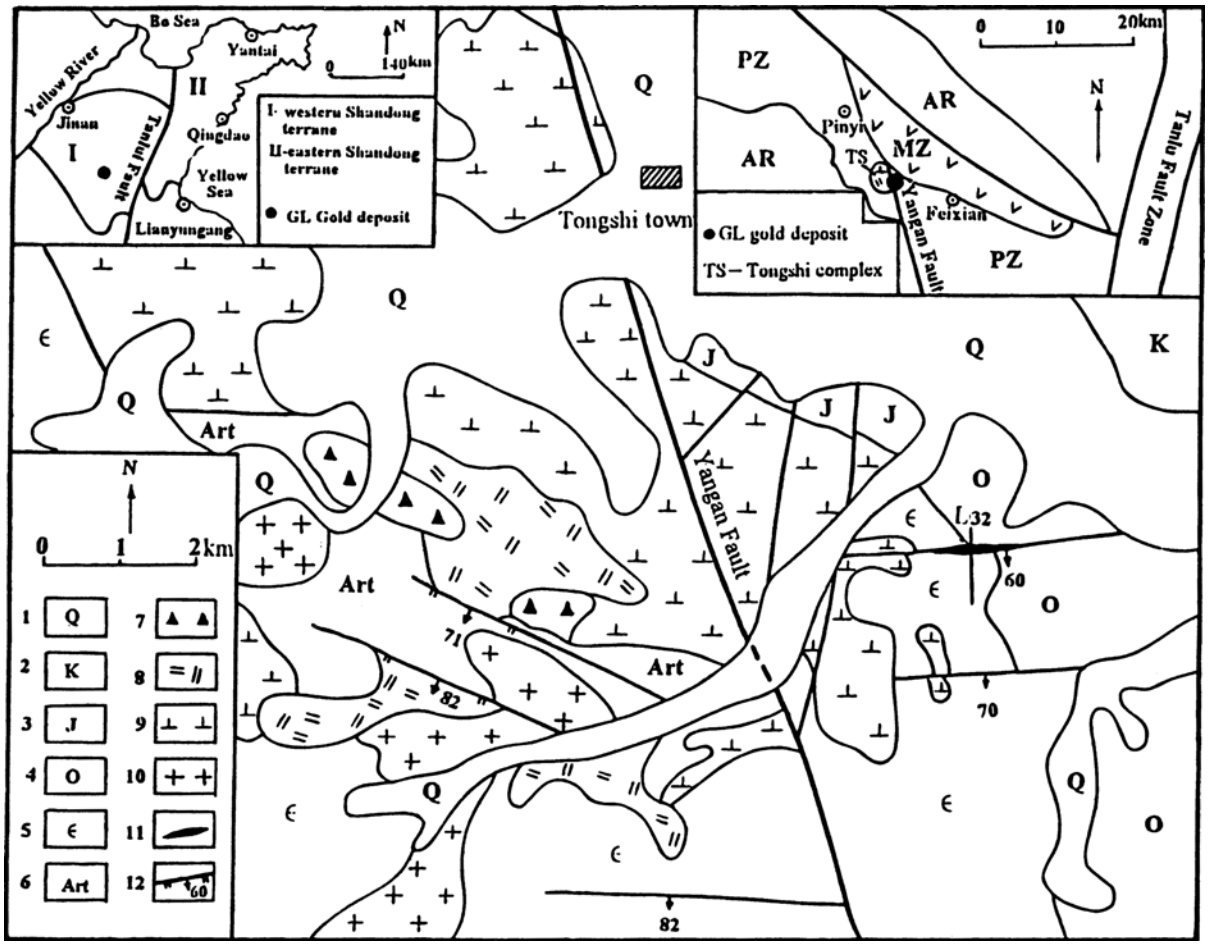

Figure 1. Geological map of the Guilaizhuang gold district. [GL, Guilaizhuang gold deposit; AR, Archean metamorphic terrane; PZ, Paleozoic sedimentary terrane; MZ, Mesozoic volcanic terrane; L_{32}, No. 32 exploratory survey line; 1, Quaternary sediments; 2, Cretaceous volcanic sedimentary rocks; 3, Jurassic volcanic sedimentary rocks; 4, Ordovician carbonate rocks; 5, Cambrian carbonate rocks; 6, Archean metamorphic rocks; 7, Cryptobreccia; 8, Mesozoic diorite-porphyrite; 9, Mesozoic syenite-porphyry; 10, Archean granodiorite; 11, Guilaizhuang gold deposit; 12, Fault and its attitude].

zonation of the primary halos associated with the Guilaizhuang deposit and to establish a geochemical prospecting pattern.

GEOLOGICAL FEATURES

The deposit is localized in a cryptobreccia zone controlled by east-west-trending faults about 1 km east from the Tongshi subvolcanic alkalic intrusive complex. The complex consists of hypabyssal suites of diorite-porphyrite and syenite-porphyry enriched in K_2O (4.06–10.12%) and Au (5.40–12.46 ppb). Two $^{40}Ar/^{39}Ar$ analyses of amphiboles from the diorite-porphyrite and the syenite-porphyry suites have recorded ages of 189 and 188 Ma, respectively (Yu, 1996). It is inferred from the isotopic ages and the intersections of the intrusive bodies that the diorite-porphyrite suite solidified earlier than the syenite-porphyry suite. Exposed rocks in the mine are mainly Archean metamorphic rocks (Au, 10.14 ppb, based on 186 samples), Cambrian and Ordovician limestones (Au, 4.13 ppb, based on 30 samples) and dolomite (Au, 12.81 ppb, based on 24 samples). The main host

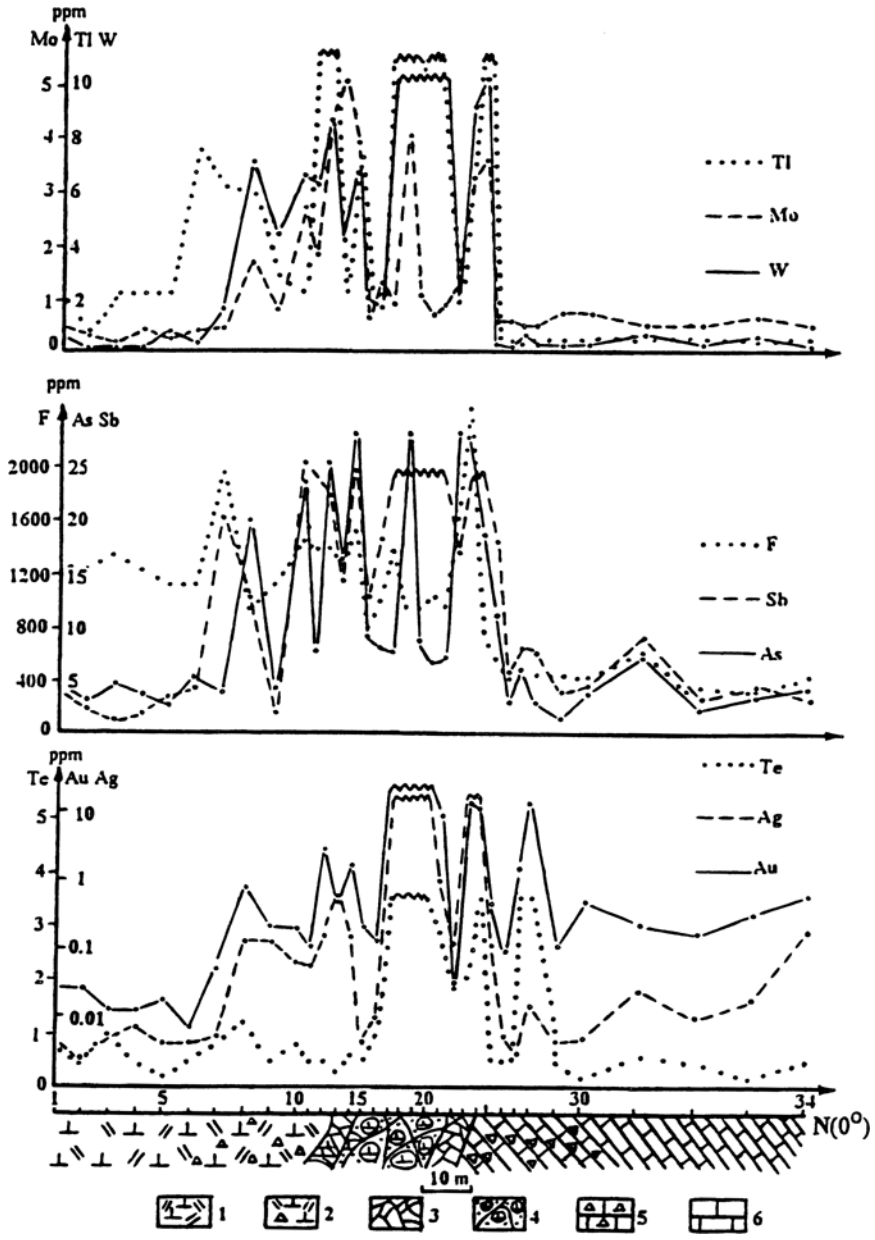

Figure 2. A geological-geochemical cross-section of the Guilaizhuang gold deposit, showing the transverse zonation of the indicator elements in primary halos and the zonation of the cryptobreccia. [1, syenite porphyry; 2, fissure syenite porphyry; 3, cataclasite; 4, breccia ore body; 5, fissure carbonate rocks; 6, carbonate rocks].

rocks are limestone and dolomite. The composition of the breccia zone is complex (diorite-porphyrite dikes, syenite-porphyry dikes, carbonate rocks as well as metamorphic rocks) and zoned. From the center of the zone toward the hanging wall and the foot wall, the zonation is as follows: breccia ⇒ cataclastite ⇒ fissure rock ⇒ normal rock. The mineralization as well as the alteration varies from intensive to weak as indicated in figure 2. Ore-forming processes occurred at the end of the magmatic cycle and were associated with the cryptobrecciation caused by the activities of east-west-trending faults. The alteration minerals are potash feld-

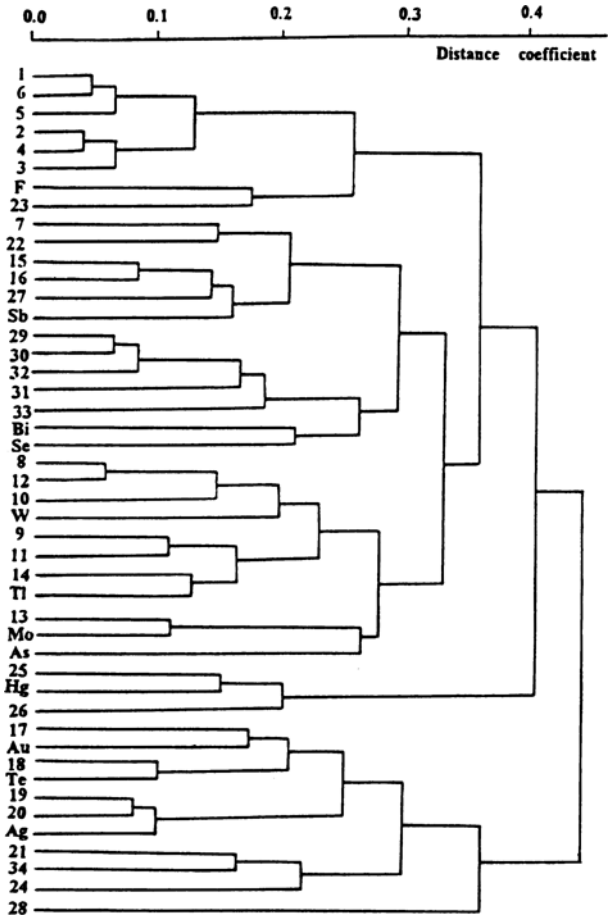

Figure 3. The correspondence cluster dendrogram of the Guilaizhuang gold deposit, indicating the transverse zonation of element association in primary halos (sample numbers are the same as figure 2).

spar, fluorite, quartz, arsenopyrite, scheelite, and roscoelite. The ore minerals are mainly native gold, electrum, and calaverite.

ZONATION IN PRIMARY HALOS

Transverse Zonation

Transverse zonation in primary halos may reflect differences of mineralization across the orebody. The characteristics of the zonation depend on the concentration of elements in the orebody, in the halos, and the relative mobility of elements, as well as on the background content of elements in the enclosing rocks (Beus and Grigorian, 1977). The zonation of the deposit is shown in figure 2. Thirty-four samples were collected across the main orebody. Analyses of Au, Ag, Te, As, Sb, F, W, Mo, and Tl show clear anomalies within the orebody and its enclosing rocks (table 1, fig. 2). The anomalies are ranked in decreasing order according to the width of the anomaly: Au, Ag > F, As, Sb, Tl > W, Mo > Te. The elements' mobility decreases from Au to Te as indicated in figure 2.

Correspondence cluster analysis (Ji and others, 1993) further revealed the zonation of element associations as shown in figure 3. The samples and elements are classified into two groups: an Au–Ag–Te ore-forming element group (sample numbers 17, 18, 19, 20, 21, 24, and 28) and an alteration element group. The latter is further divided into three sub-groups: F (fluoritization, sample numbers 1, 2, 3, 4, 5, 6, and 23); W–Mo–As–Tl (sample numbers 8, 9, 10, 11, 12, 13, and 14); and Se–Sb–Bi (sample numbers 7, 15, 16, 22, 27, 29, 30, 31, 32, and 33). The zonation of element groups is as follows: (the hanging wall) F ⇐ W–Mo–As–Tl ⇐ Se–Sb–Bi ⇐ (orebody) Au–Ag–Te ⇒ Se–Sb–Bi (the foot wall).

Axial Zonation

Axial zonation is expressed in the direction of movement of ore-bearing solutions. A total of 131 samples collected from five drill cores were used for the analysis of the axial zonation. Nineteen variables including Au, Ag, W, Mo, F, As, Sb, Te, Tl, Cu, Pb, Zn, Cr, Ni, Co, V, SiO_2, K_2O, and Na_2O were analyzed for each sample and plotted in cross-section shown in figure 4. There are obvious anomalies of Au, Ag, As, Sb, W, Mo, F, Tl, V, and Zn within the orebody and the enclosing rocks. The anomalies are controlled by the cryptobreccia zone. The values of Au and Tl abruptly increase and reach a maximum of 132.5 ppm and 190.0 ppm, respectively, near the intersection of the cryptobreccia and the syenite-porphyry dike. The same is true for F. This suggests that the deposition of the ore shoots is closely associated with the activities of the dike rocks. The primary halos of indicator elements such as Au, Ag, and Sb nearly coincide with the orebody and are wider and more pronounced in the upper portion of the section. The halos gradually narrow along the edges of the deposit. The halos of Ag and Sb become intensive again at depth, which suggests the presence of another deeper orebody. The halo of As expands with depth. The halos of W and Tl are the widest and most pronounced in the middle portion of the section and gradually narrow upwards

Table 1. Concentration Values of Trace Elements in Rock Samples[a]

Sample no.	Au	Ag	As	Sb	Bi	Hg	W	Mo	Se	Te	F	Tl
1	0.006	0.047	4.43	1.66	0.15	0.026	0.55	0.47	0.51	0.18	1200	11.00
2	0.006	0.032	3.26	0.94	0.36	0.031	0.04	0.28	0.51	0.15	1200	3.80
3	0.004	0.056	4.69	0.51	0.19	0.023	0.04	0.09	0.41	0.20	1350	11.30
4	0.004	0.062	3.61	0.65	0.18	0.028	0.06	0.38	0.32	0.15	1200	11.00
5	0.005	0.044	2.72	1.29	0.06	0.024	0.75	0.27	0.37	0.12	1020	11.60
6	0.003	0.044	5.26	1.74	0.30	0.028	0.23	0.38	0.37	0.15	1020	37.50
7	0.009	0.050	3.87	8.06	0.24	0.033	1.54	0.40	0.32	0.18	1860	31.00
8	0.040	0.260	19.30	5.51	0.30	0.031	7.03	2.66	0.51	0.22	930	29.50
9	0.019	0.300	3.90	1.64	0.20	0.029	4.02	0.76	0.46	0.15	1080	14.00
10	0.018	0.200	23.00	9.77	0.28	0.043	6.53	2.66	0.46	0.18	1530	11.10
11	0.014	0.180	7.65	3.37	0.02	0.045	6.03	1.75	0.41	0.15	1440	60.40
12	0.078	0.320	24.80	8.56	0.64	0.064	8.54	4.18	0.38	0.15	1440	58.00
13	0.030	0.400	15.90	5.74	0.48	0.040	4.08	5.69	0.41	0.13	1200	11.20
14	0.060	0.320	53.00	26.80	0.79	0.101	6.59	3.80	0.55	0.16	1530	37.50
15	0.018	0.044	7.59	5.09	0.12	0.062	1.88	0.57	0.46	0.15	750	11.30
16	0.015	0.072	7.77	7.33	0.11	0.048	1.57	1.33	0.46	0.20	1080	11.00
17	2.864	3.39	7.41	29.90	0.18	0.131	28.90	0.85	0.37	3.34	1440	92.00
18	4.550	4.82	147.00	99.80	0.98	0.175	15.10	3.95	0.41	13.90	930	82.20
19	2.038	3.81	8.53	19.60	0.66	0.075	16.60	0.99	0.32	5.23	930	52.00
20	3.097	6.20	6.41	20.00	0.41	0.096	12.80	0.68	0.41	4.07	1020	74.00
21	0.151	0.91	6.70	17.80	0.47	0.057	12.80	0.84	0.46	0.31	930	31.00
22	0.006	0.26	37.70	6.61	0.58	0.048	1.88	1.29	0.74	0.18	1530	11.20
23	0.685	1.61	38.60	34.00	0.55	0.079	9.04	3.11	0.60	0.22	4350	28.60
24	0.202	2.68	18.50	49.70	0.59	0.124	12.6	3.49	0.46	2.06	720	72.30
25	0.029	0.26	10.70	6.97	0.24	0.477	0.16	0.47	0.46	0.15	465	1.32
26	0.012	0.050	2.58	2.24	0.14	0.146	0.04	0.52	0.41	0.15	240	0.38
27	0.052	0.036	5.88	3.37	0.06	0.071	0.60	0.45	0.37	0.44	510	1.75
28	0.791	0.090	2.80	2.89	0.23	0.123	0.19	0.47	0.41	0.73	261	0.39
29	0.013	0.045	1.68	1.51	0.10	0.100	0.10	0.66	0.37	0.15	249	0.42
30	0.019	0.050	3.81	1.64	0.22	0.085	0.06	0.66	0.32	0.11	210	0.11
31	0.020	0.12	7.33	3.64	0.10	0.130	0.54	0.48	0.37	0.16	345	0.40
32	0.016	0.072	2.29	1.29	0.16	0.066	0.13	0.45	0.32	0.15	162	0.41
33	0.025	0.10	3.62	1.75	0.29	0.059	0.48	0.57	0.41	0.12	147	0.39
34	0.033	0.38	4.37	1.21	0.24	0.032	0.10	0.47	0.36	0.15	228	0.40
Technique	GFAAS	AAS	AFS	AFS	AFS	AFS	PL	PL	PL	PL	SE	AES
Detection limit	0.1[2]	0.01[1]	0.01[1]	0.03[1]	0.03[1]	0.02[2]	0.05[1]	0.01[1]	0.05[1]	0.05[1]	20[1]	0.05[1]

[a] Values expressed in ppm; detection limit expressed in: 1, ppm; 2, ppb.

and downwards. The halos of F and Mo are small but gradually become more pronounced at depth. The halo of Zn is the weakest.

The zonation indexes of indicator elements were calculated by using S. V. Grigorian's method (Beus and Grigorian, 1977). The zonation sequence of indicator elements, according to the zonation index (see table 2) is as follows:

$$\text{Au} \Rightarrow (\text{Sb, Ag, Zn, V}) \Rightarrow \text{W} \Rightarrow (\text{Mo, F, Tl, As})$$

A detailed sequence of indicator elements was obtained by using the variability index of indicator elements as follows:

$$\text{Au} \Rightarrow \text{Ag} \Rightarrow \text{Sb} \Rightarrow \text{V} \Rightarrow \text{Zn} \Rightarrow \text{W} \Rightarrow \text{F} \Rightarrow \text{Mo} \Rightarrow \text{Tl} \Rightarrow \text{As}$$

EVALUATION CRITERIA FOR ORE POTENTIAL AT DEPTH

Methods for interpretating geochemical anomalies in the search for blind mineralization should be considered together with the assessment of ore potential at depth in those places where ore mineralization appears at the surface (Beus and Grigorian, 1977). The evaluation criteria using indicators for gold are listed

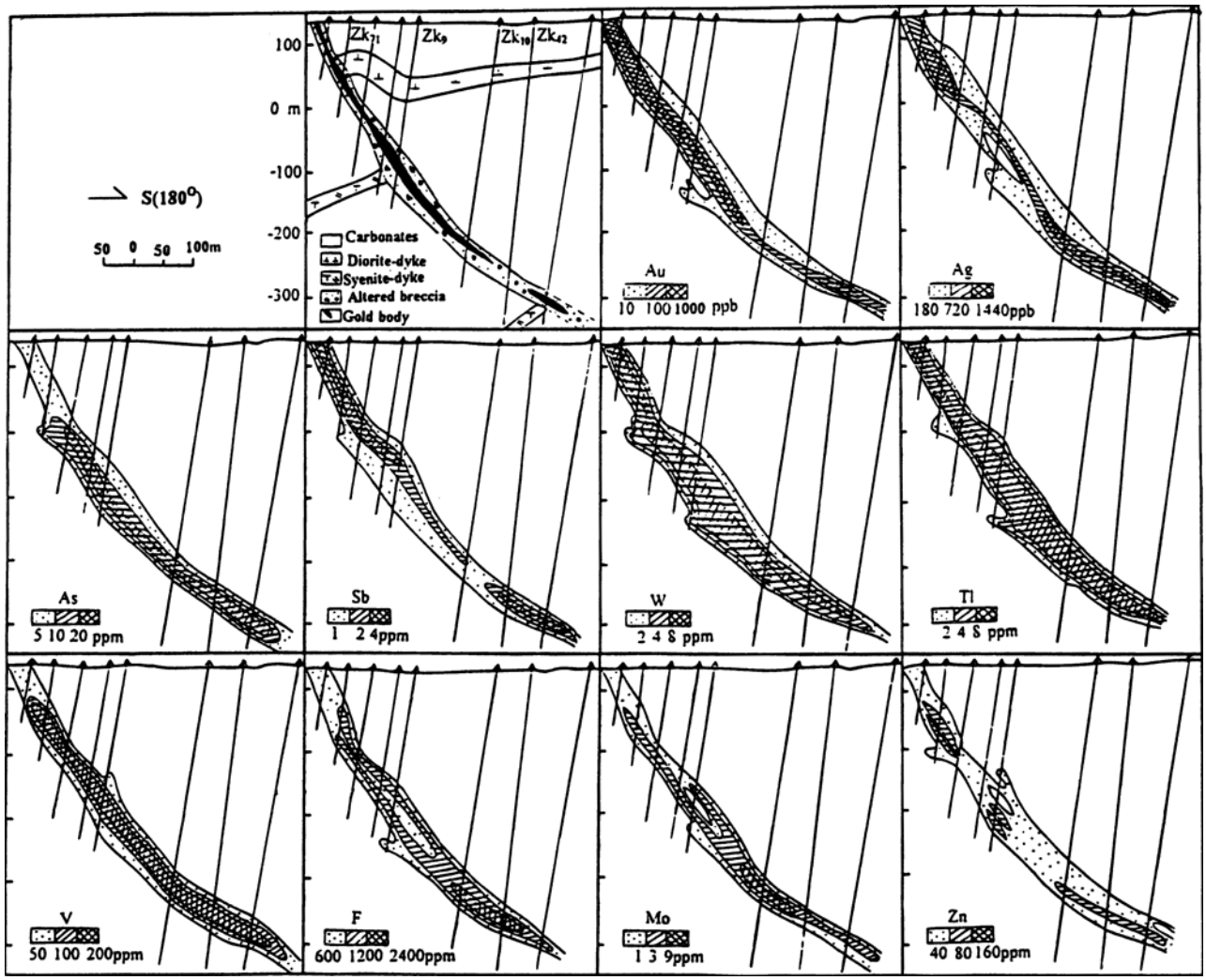

Figure 4. Primary geochemical anomaly cross-sections of the No. 32 exploratory survey line in the Guilaizhuang gold district, showing the axial zonation of the indicator elements in primary halos.

Table 2. Zonation Indexes of Indicator Elements

Altitude (m)	Au	Ag	As	Sb	W	Mo	Zn	F	Tl	V
50	0.260	0.110	0.020	0.014	0.040	0.087	0.183	0.210	0.038	0.043
0	0.016	0.122	0.074	0.108	0.053	0.069	0.269	0.163	0.077	0.050
−50	0.006	0.012	0.079	0.019	0.139	0.066	0.196	0.258	0.164	0.046
−200	0.003	0.021	0.034	0.003	0.020	0.180	0.145	0.355	0.221	0.019
−300	0.020	0.250	0.154	0.012	0.120	0.055	0.184	0.106	0.072	0.032

Table 3. Criteria for the Search for Blind Mineralization and the Assessment of Ore Potential at Depth[a]

Altitude (m)	$\frac{(Au \cdot Ag)_D}{(As \cdot Tl)_D}$	$\frac{(Au)_D}{(Tl)_D}$	$\frac{(Au)_D}{(As)_D}$	$\frac{(Au+Ag)_D}{(As+Tl)_D}$	$\frac{(Au+Sb)_D}{(As+Tl)_D}$
50	32.00	6.84	13.00	6.38	4.70
0	0.34	0.21	0.22	0.91	0.82
−50	5.1×10^{-3}	0.04	0.08	0.07	0.10
−200	7.7×10^{-3}	0.01	0.09	0.09	0.02
−300	0.45	0.28	0.13	1.19	0.14

[a] Calculated by using the zonation indexes of table 2: 1, the ratios of zonation index of indicator elements; 2, the ratios of multiplicative zonation index of indicator elements; 3, the ratios of additive zonation index of indicator elements.

in table 3. These indexes decrease rapidly from the upper portion of the orebody to the lower portion but increase abruptly at the edges.

ORE (HALO)-FORMING MECHANISM

The 131 samples mentioned earlier were further examined by means of factor analysis. The orthogonal rotation factor loadings are listed in table 4. Taking 0.6 as the threshold value, the following factors were identified:

- F_1 [Au, Ag, Sb, V]: association of native gold, electrum, calaverite, and roscoelite, which reflects the element concentrations derived from epithermal ore-forming liquids.
- F_2 [Ni, Cu, Mo]: association of sulfide of Ni, Cu, Mo, (Fe), and so forth, which reflects the element concentrations derived from mesothermal ore-forming liquids.
- F_3 [Co, Zn]: association of sulfide of Zn and Co, which also reflects the element concentrations derived from mesothermal ore-forming liquids.
- F_4 [W, Tl, As]: association of arsenopyrite and scheelite, which reflects the element concentrations derived from xenothermal liquids.
- F_5 [K_2O, SiO_2, Na_2O, F]: alteration association of potash feldspar, albite, and fluorite which reflects the alteration minerals formed by reactions with xenothermal liquids.

Table 4. Orthogonal Rotation Factor Loadings[a]

Variable	F1	F2	F3	F4	F5
Au	**0.8650**	−0.0456	0.0655	0.0435	0.1435
Ag	**0.8889**	0.0359	−0.1956	0.0850	0.0858
W	0.1556	0.0468	0.0528	**0.8423**	0.1111
Mo	0.1868	**0.6195**	0.3046	0.1509	0.4779
F	0.0943	0.0326	−0.1274	0.3443	**0.7640**
As	0.2308	0.2277	−0.3210	**0.7226**	0.1867
Sb	**0.7464**	0.0232	−0.3068	0.3729	0.1666
Tl	0.0660	−0.0235	0.0912	**0.8305**	0.3605
SiO_2	0.3785	0.0842	−0.1402	0.1336	**0.8544**
K_2O	0.1918	0.0230	−0.1835	0.1876	**0.8782**
Na_2O	0.0585	0.4933	0.1835	0.0075	**0.7188**
Cr	0.5842	0.2279	−0.3868	0.0325	0.4588
Ni	−0.0540	**0.8598**	−0.2173	0.1738	−0.0329
Co	−0.0412	0.2996	**−0.8790**	0.0300	0.1869
V	**0.8828**	0.0910	0.0087	0.1820	0.3374
Cu	0.0543	**0.8320**	−0.1054	−0.0482	0.0829
Pb	0.3342	−0.0285	−0.3614	0.2955	0.7241
Zn	0.2123	0.0630	**−0.8448**	−0.0098	0.1017
Eigenvalue	7.3293	2.3036	1.9669	1.5978	1.4336
Cumulative percentage	40.7185	53.5162	64.4433	73.3198	81.2842

[a] Values in boldface are values above the threshold value of 0.6.

According to the above analyses, the ore (halo)-forming process may be divided into two stages: an alteration stage and a mineralization stage. The former includes potash feldsparization, albitization, and fluoritization. The latter includes three substages: arsenopyritization and scheelitization; sulfides of Fe, Cu, and Zn; and native gold, electrum, and calaveritization. The last substage is considered to be the main ore-forming stage. The process overall is considered to have taken place in order of decreasing temperature.

GEOCHEMICAL PROSPECTING PATTERN

Based on the results of this study, the geochemical prospecting pattern is summarized in figure 5. The orebody is located in the cryptobreccia zone within mainly carbonate rocks. The ore shoots are spatially related with alkalic dike rocks. The transverse zonation

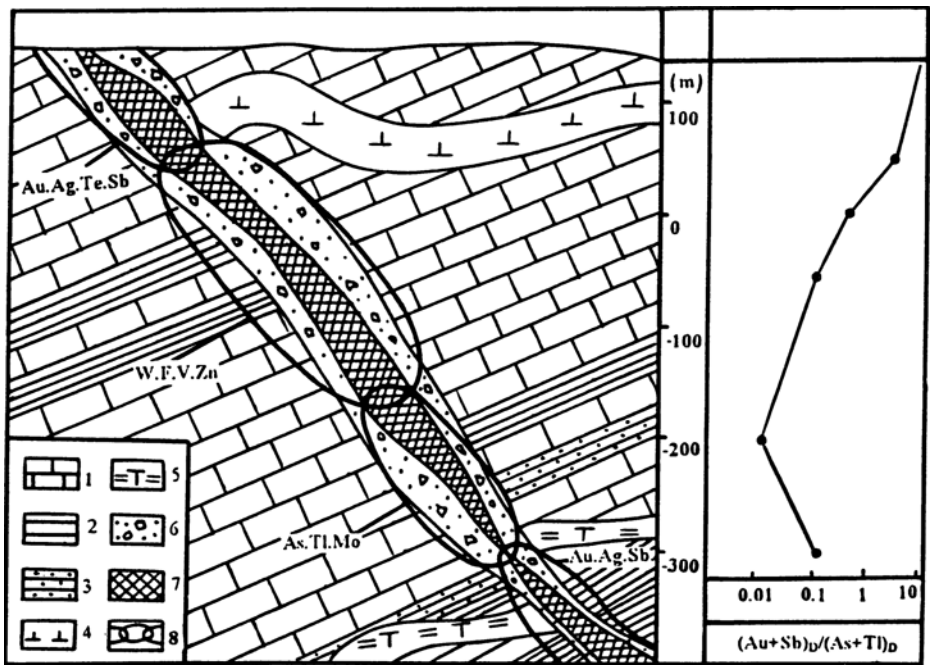

Figure 5. Geochemical prospecting pattern of the Guilaizhuang gold deposit. [$(Au + Sb)_D/(As + Tl)_D$, the ratios of additive zonation indexes of indicator elements; 1, carbonate rocks; 2, shale; 3, siltstone; 4, diorite-porphyrite; 5, syenite porphyry; 6, cryptobreccia; 7, orebody; 8, zonation of halos].

is: (the hanging wall) F ⇐ W–Mo–As–Tl ⇐ Se–Sb–Bi ⇐ Au–Ag–Te (orebody) ⇒ Se–Sb–Bi (the foot wall). The axial zonation is: Au ⇒ Ag ⇒ Sb ⇒ V ⇒ Zn ⇒ W ⇒ F ⇒ Mo ⇒ Tl ⇒ As. The ratios of indexes such as $(Au + Sb)_D/(As + Tl)_D$ decrease with depth. The values are greater than 4.0 in the upper portion, 4.0 to 0.8 in the middle portion, and 0.8 to 0.01 in the lower portion of the orebody. The values increase to 0.1 at the edges of the orebody indicating that more orebodies may exist at greater depth.

ACKNOWLEDGMENTS

Sincere appreciation is expressed to the National Nature Science Fund Commission of China for the funding in support of this research project. The authors wish to thank Dr. G. C. Pan and Dr. Q. M. Cheng for their insightful comments.

REFERENCES

Beus, A. A. and Grigorian, S. V., 1977, Geochemical Exploration Methods For Mineral Deposits: Calgary, Applied Publishing p. 92–98.

Chen, Y. Q., Ji, H. J., and Li, S. Q., 1995, Geochemical prospecting pattern of Tongshi gold field, eastern China: Geology & Prospecting, v. 31, n. 6, p. 49–53 (in Chinese).

Ji, H. J., Wu, X. S., and Chen, Y. Q., 1993, Correspondence cluster analysis: Journal of Changchun University of Earth Sciences, v. 23, n. 4, p. 459–464 (in Chinese).

Jin, L. Y., and Shen, K., 1995, Ore composition and genesis of the Guilaizhuang gold deposit in Pingyi, Shandong province: Geology of Shandong, v. 11, n. 1, p. 30–40 (in Chinese).

Li, H. F., 1995, A preliminary study of "three-stages & two series" prospecting model in Dongping gold deposit: Gold Geology, v. 1, n. 1, p. 42–45 (in Chinese).

Li, W. D., 1986, A discussion on a new type of gold deposit at the International Volcanology Symposium in New Zealand: External Volcanic Geology, v. 2, p. 1–18 (in Chinese).

Lin, J. Q., Tan, D. J., and Yu, X. F., 1995, Genesis and metallogenic model of Guilaizhuang gold deposit: Journal of Changchun University of Earth Sciences, v. 25, n. 3, p. 286–293 (in Chinese).

Qiu, J. S., Wang, D. Z., and Zhu, X. Y., 1994, The first example of Te-Au type epithermal deposit in China—The Guilaizhuang gold deposit: Geology & Prospecting, v. 30, n. 1, p. 7–12 (in Chinese).

Quan, Z. W., 1992, Ore-forming geological characteristics of Guilaizhuang gold deposit: Geological information of Shandong, v. 76, n. 2, p. 18–26 (in Chinese).

Richards, J. P., and Ledlie, I., 1993, Alkalic intrusive rocks associated with the Mount Kare gold deposit, Papua New Guinea: Comparison with the Porgera intrusive complex: Economic Geology, v. 88, n. 4, p. 755–781.

Xiang, S. Y., and Ye, J. L., 1995., A new type of gold deposit related to alkalic intrusive rocks: Mineral Resources & Geology, v. 9, n. 46, p. 73–76 (in Chinese).

Yu, X. F., 1996, Geological characteristics and genesis of the Guilaizhuang gold deposit, *in* Shandong Bureau of Geology & Mineral Resources, ed., Proceedings of researches on the geology & mineral resources in Shandong province: Jinan, Shandong Science & Technology Press, p. 129–139 (in Chinese).